Bright hybrid white light-emitting quantum dot device with direct charge injection into quantum dot*

Jin Cao(曹进)[2,†], Jing-Wei Xie(谢婧薇)[1], Xiang Wei(魏翔)[2], Jie Zhou(周洁)[2], Chao-Ping Chen(陈超平)[3], Zi-Xing Wang(王子兴)[2], and Chulgyu Jhun(田哲圭)[4]

[1] *School of Materials Science and Engineering, Shanghai University, Shanghai* 200072, *China*
[2] *Key Laboratory of Advanced Display and System Applications, Ministry of Education, Shanghai University, Shanghai* 200072, *China*
[3] *National Engineering Laboratory of TFT-LCD Materials and Technologies, Department of Electronic Engineering, Shanghai Jiao Tong University, Shanghai* 200240, *China*
[4] *School of Green Energy & Semiconductor Engineering, Hoseo University, Asan City, Chungnam*, 336-795, *South Korea*

(Received 8 June 2016; revised manuscript received 8 August 2016; published online 25 October 2016)

A bright white quantum dot light-emitting device (white-QLED) with 4-[4-(1-phenyl-1H-benzo[d]imidazol-2-yl)phenyl]-2- [3-(tri-phenylen-2-yl)phen-3-yl]quinazoline deposited on a thin film of mixed green/red-QDs as a bilayer emitter is fabricated. The optimized white-QLED exhibits a turn-on voltage of 3.2 V and a maximum brightness of 3660 cd/m^2@8 V with the Commission Internationale de l'Eclairage (CIE) chromaticity in the region of white light. The ultra-thin layer of QDs is proved to be critical for the white light generation in the devices. Excitation mechanism in the white-QLEDs is investigated by the detailed analyses of electroluminescence (EL) spectral and the fluorescence lifetime of QDs. The results show that charge injection is a dominant mechanism of excitation in the white-QLED.

Keywords: quantum dot light-emitting devices, white, ultra-thin film, charge injection

PACS: 85.60.Jb, 78.67.Hc, 78.20.–e, 61.46.Df **DOI:** 10.1088/1674-1056/25/12/128502

1. Introduction

Colloidal quantum dots (QDs) are attractive luminescent materials for creating light-emitting diodes (QLEDs) applying to display or solid-state lightings due to their characteristics of size-tunable band gap, high photoluminescence (PL) quantum yield (QY), good stability and saturated colors with a narrow bandwidth.[1–4] Since the first QLEDs were demonstrated in 1994,[5] the monochrome device performances have steadily improved in terms of the brightness (21800 cd/m^2),[6] current efficiency (40 cd/A),[7] external quantum efficiency (20.5%), and device lifetime (10^5 hours).[8] Recently, white-QLEDs have also received extensive attention as a cost-competitive energy-efficient alternative to conventional electrical lighting. Several researchers have reported the use of a stacked structure of QDs and polymers or the hybridization of QDs/polymers as emissive layer (EML) for enhancing efficiency and obtaining color tuning capability.

Prototype results from the direct electroluminescence (EL) of QDs through integrating red, green, and blue emitting QDs to produce white-QLEDs have been demonstrated.[9,10] However, the use of blue-QDs can lead to reduced brightness and efficiency because blue-QDs inherently possess unfavorable energy level rendering hole injection into them from neighboring hole transport layer (HTL) inefficient. Tan *et al.*[11] reported the white-QLEDs with a bilayer structure of yellow-QDs/poly(N, N'-bis(4-butylphenyl)-N, N'-bis(pheny)benzidine) (Poly-TPD). However, the available blue-emitting polymer with high luminescent efficiency and chemical resistance to adjacent layers is highly limited. Kang, *et al.*[12] reported that the white-QLEDs by using the hybridization of poly(9,9-dioctylfluorenyl-2, 7-diyl) (PFO) blended with red- and green-colored CdSe@ZnS QDs as EML, exhibited the Commission Internationale de l'Eclairage (CIE) 1931 chromaticity of (0.33, 0.36) and maximun brightness of 1163 cd/m.[2] Torriss *et al.*[13] realized the white-QLEDs by using red-QDs and blue organic molecule iridium(III)bis(2-(4,6-difluorephenyl) pyridinato-N,C2) (Ir(III)DP) dispersed into poly(N-vinylcarbazole) (PVK) as EML. Wu *et al.*[14] reported white-QLEDs with red-QDs and 4, 4-bis(2,2-diphenylethen-1-yl) biphenyl (DPVBi) dispersed into PVK as EML. In the above cases, the multi-color emitters (QDs and/or organic molecule) are blended into a single EML and interact in a non-trivial way. Then those devices suffer low luminance and high operating voltage due to the high concentration of the mixed materials.[15,16]

In this paper, we propose a white-QLED using a blue fluorescent material 4-[4-(1-phenyl-1H-benzo[d]imidazol-2-yl)phenyl]-2-[3-(tri-phenylen-2-yl)phen-3-yl]quinazoline (BITpQz) deposited over the mixed green- and red-QDs layer to create a bilayer EML. With the ignorable influence of BiTpQz on the PL lifetime of QDs, a stable and bright white-

*Project supported by the National Natural Science Foundation of China (Grant No. 21302122) and the Science and Technology Commission of Shanghai Municipality, China (Grant No. 13ZR1416600).

†Corresponding author. E-mail: cj2007@shu.edu.cn

© 2016 Chinese Physical Society and IOP Publishing Ltd

QLED operation in a wide range of bias is obtained by controlling the ratio between green-QDs and red-QDs under the critical condition of ultra-thinness. The turn-on voltage (the voltage at brightness of 1 cd/m^2) of the white-QLED is as low as 3.2 V, and the maximum brightness is measured to be 3660 cd/m^2. Detailed spectral analysis is presented, and the results show that charge injection appears to be an important mechanism of EL in our device.

2. Experimental details

2.1. Materials

In the present study, QD synthesis was carried out by using the following reagents: Cadmium oxide (CdO, powder, 99.99%), zinc acetate ($Zn(AC)_2$, solid, 99.9%), selenium powder (Se, powder, 99.99%), sulfur powder (S, powder, 99.9%), oleic acid (OA, 90%), trioctylphosphine (TOP, 90%), 1-octadecene (ODE, 90%). All chemicals were purchased from Sigma Aldrich. According to the processes of Ref. [17], we obtained the CdSe-ZnS core-shell QDs with PL wavelengths of 515 nm (green) and 651 nm (red), QYs of 90% (green) and 70% (red), full width at half maximum (FWHM) of 38 nm (green) and 34 nm (red), respectively. The transmission electron microscope (TEM) results of green-QDs and red-QDs are shown in the inset of Fig. 1(a). It can be seen that the regular sphere of green-QDs ($\sim$ 7 nm) and the irregular polygon of red-QDs ($\sim$ 10 nm) have been obtained. The

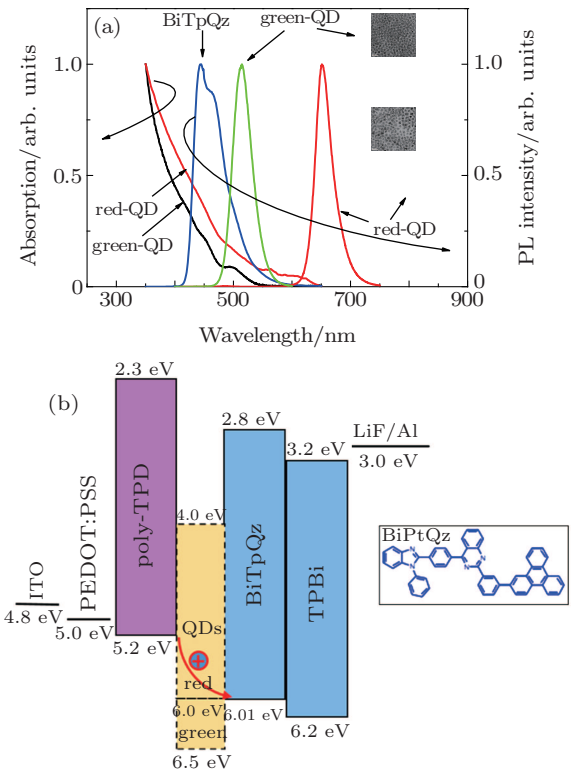


Fig. 1. (color online) (a) Normalized PL spectra of the QDs, BiTpQz, and absorption spectra of QDs with the inset: TEM results of the QDs. (b) Energy band diagram of the proposed white-QLED and the chemical structure of BiTpQz.

different shapes between green and red QDs are possible due to a longer synthetic time ($\sim$ 20 min) of red-QDs than the green-QDs ($\sim$ 10 min). The blue organic material BITpQz with a PL wavelength of 445 nm, the highest occupied molecular orbital (HOMO) level of 6.01 eV, and the lowest unoccupied molecular orbital (LUMO) level of 2.8 eV was purchased from YuRui Chemical Company in Shanghai, China. The PL and absorption spectra of QDs and BITpQz are shown in Fig. 1(a). The molecular structure of BiTpQz and energy level alignments are shown in Fig. 1(b).

2.2. Film and device fabrication

The various layers of QLEDs in this work were fabricated by a combination of solution-processing and vacuum evaporation techniques. All the solution processes were performed in an N_2 filled glovebox with the H_2O and O_2 below 10 ppm. Firstly, the glass substrate precoated with a 150-nm thick, $\sim$ 10 Ω/sq indium tin oxide (ITO) layer was degreased in an ultrasonic bath by the following sequence: in detergent, deionized water, acetone, and isopropanol, and then cleaned in a UV-ozone chamber for 15 min. After being cleaned, the hole injection layer (HIL) of poly(3,4-ethylenedioxythiophene)-poly(styrenesulfonate) (PEDOT:PSS) was spin-deposited onto ITO by a spin coater with a speed of 5000 rpm and heated at 150 °C for 30 min. HTL of poly-TPD was spin-coated onto PEDOT:PSS with a speed of 3000 rpm and heated at 110 °C for 60 min. Then, the QDs were spin-coated onto poly-TPD with a speed of 1500 rpm and dried at 150 °C for 30 min to form the first EML. After spin-coating processing, the blue emitting layer of BiTpQz was thermally evaporated on QDs in a high vacuum ($\sim 10^{-4}$ Pa) chamber to form the second EML. Finally, the electron transfer layer (ETL) of 1,3,5-tris(2-phenyl-1H-benzo[d]imidazol-1-yl)benzene (TPBi), electron injection (EIL) of lithium fluoride (LiF), and the cathode of aluminum (Al) were deposited sequentially in the same chamber without breaking the vacuum. The thickness values and the deposition rates of the materials were monitored in situ by an oscillating quartz thickness monitor. The typical deposition rates for organic materials, LiF, and Al were 0.5, 0.1, and 5.0 Å/s, respectively. The device active areas defined by the overlap between the electrodes were 3 mm×3 mm in all cases. For the time-resolved photoluminescence (TRPL) measurements, the QDs/BiTpQz blend films were deposited on quartz substrates by using QD and BiTpQz mixed solutions with a mole ratio of about 1/2000 by a spin coater with a speed of 500 rpm. The QD concentrations in these blend films were low in order to avoid aggregating QDs and reduce the influence of the QDs/BiTpQz mole ratio on the energy transfer rate.[18] The QDs/poly(methyl methacrylate) (PMMA) blend film and the QDs in toluene solution were prepared as reference samples.

The luminescence–voltage–current density (*L*–*V*–*J*) characteristics of devices were measured simultaneously with Keithley 2400 source meter and Minolta L110 luminance meter at room temperature. The EL spectra were measured with the PR650 spectrometer. All devices were measured immediately under ambient atmosphere without being encapsulated after the devices had been fabricated. The absorption spectra were measured by a HITACHI U-3900H spectrophotometer. The TRPL spectra were measured by FL920 fluorescence lifetime spectrometer. The excitation source was a hydrogen flash lamp (nF900) with a pulse width of 1.5 ns and a picosecond pulsed diode laser (EPL-485) with a pulse width of 85 ps.

3. Results and discussion

The energy level diagram of the white-QLEDs is shown in Fig. 1(b). The work functions of ITO anode and LiF/Al cathode, the QDs conduction/valance band, and the HOMO/LUMO of organic materials are cited from Refs. [19] and [20]. It can be seen from Fig. 1(b) that holes and electrons can be injected without facing energy barrier until they reach poly-TPD/QD interfaces from PEDOT:PSS to poly-TPD and from BiTpQz to QDs, respectively. When the voltage is increased to the turn-on voltage, holes can be injected into red-QDs and/or BiTpQz from poly-TPD to form excitons. It is worth noting that the ultra-thin layer of QDs is critical for the blue light generation in the device as proved below. Then, as the voltage increases continuously, the holes can be injected into green-QDs from poly-TPD and generate the white emission. The detailed process in the white-QLED operation will be discussed below.

In order to investigate the influence of the thickness of quantum dots on the performances of device, the QLEDs with only green-QDs (named device-G) and red-QDs (named device-R) instead of mixed green and red-QDs as the first EML were fabricated. The structures of device-G (the inset of Fig. 2(a)) and device-R (the inset of Fig. 2(b)) are ITO/PEDOT:PSS(20 nm)/poly-TPD(40 nm)/green-QDs/BiTpQz(20 nm)/TPBi(40 nm)/LiF(1 nm)/Al(100 nm) and ITO/PEDOT:PSS(20 nm)/poly-TPD(40 nm)/red-QDs/BiTpQz(20 nm)/TPBi(40 nm)/LiF(1 nm)/Al(100 nm), respectively. The concentrations of green-QDs in toluene solution were 2, 4, 6, and 10 mg/ml corresponding to the estimated thickness values (based on Ref. [21]) of 0.4 monolayer (ML), 0.8 ML, 1.2 ML, and 2 ML for the QD layers in device-G1, device-G2, device-G3, and device-G4, respectively. The concentrations of red-QDs in toluene solution were 6.5, 8, 9, and 13 mg/ml corresponding to the estimated thickness values of 1 ML, 1.2 ML, 1.4 ML, and 2 ML for the QD layers in device-R1, device-R2, device-R3, and device-R4, respectively. The normalized EL spectra of device-G and device-R at 9 V bias are shown in Figs. 2(a) and 2(b), respectively. The *L*–*V*–*J* characteristics of devices-G, and devices-R are shown in Figs. 2(c) and 2(d), respectively.

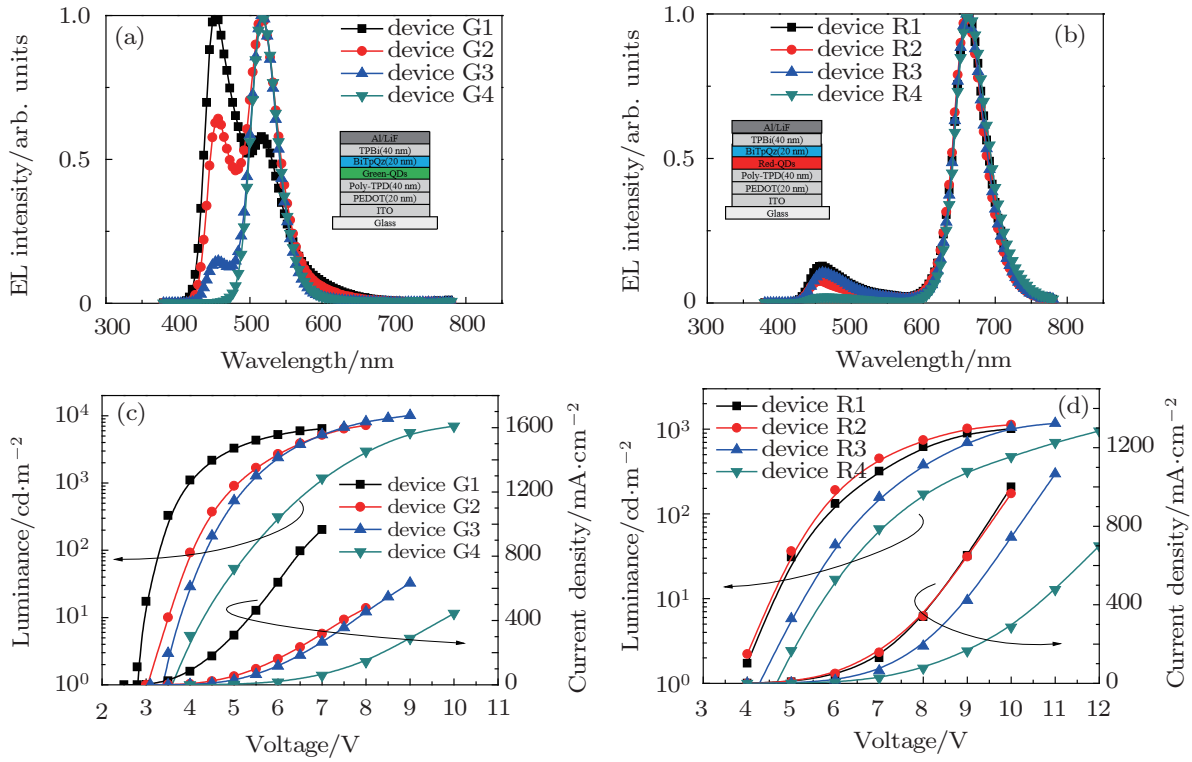


Fig. 2. (color online) Normalized EL spectra at an applied voltage of 9 V for (a) devices-G with the green-QD thickness values of 0.4, 0.8, 1.2, and 2 ML for the devices G1, G2, G3, and G4, respectively, and (b) devices R with the red-QD thickness values of 1, 1.2, 1.4, and 2 ML for the devices R1, R2, R3, and R4, respectively. The *L*–*V*–*J* characteristics of (c) devices-G, and (d) devices-R. The insets in panels (a) and (b) show the structures of devices-G and devices-R, respectively.

For device-G, figure 2(a) shows two peaks at 456 nm and 516 nm corresponding to the emissions of BiTpQz and green-QDs. With the thickness of green-QDs increasing from 0.4 ML to 2 ML, the blue color component in the spectra changes from dominance to disappearance. It indicates that blue emission can be generated easily when the QD layer is ultra-thin (less than 1 ML), but inhibited while the QDs layer is thick enough. It can be seen from Fig. 2(c) that the current density and luminance of device at the same voltage decrease with the thickness of the green-QDs increasing. It also implies that more and more QDs take part in the luminescent process, which leads to the influences of the unfavorable HOMO level of green-QDs (6.5 eV, as shown in Fig. 1(b)) getting greater and, consequently increasing the driving voltage of device-G. For device-R, figure 2(b) shows two peaks at 456 nm and 660 nm corresponding to the emissions of BiTpQz and red-QDs. As the thickness of red-QDs increases, device-R shows similar trends to device-G, the blue color component in the spectrum deceases as shown in Fig. 2(b), and the current densities and luminances of the devices at the same voltage decrease as shown in Fig. 2(d). Compared with green one, the higher ratio of QD components in spectrum of device-R can be mainly attributed to the difference in HOMO level between red-QDs (6.0 eV) and green-QDs (6.5 eV). The EL spectra in Fig. 2 is slightly redshifted from the solution PL measured in Fig. 1(a). We attribute this redshift to a combination of interdot interactions, which have been observed previously in closely packed QD solids,[22] and the electric-field-induced Stark effect.[23] From Fig. 2 we can know that the similar trends happen in device-G and device-R, and the ultra-thin layer (less than 1 ML) of QDs is critical for the efficient blue light emission in both cases.

To obtain the white-QLED, the devices (named device-W) with mixed green-QD and red-QD layer as the first EML are fabricated with a structure (upper inset of Fig. 3(c)) of ITO/PEDOT:PSS(20 nm)/poly-TPD(40 nm)/green-QDs:red-QDs/BiTpQz(20 nm)/TPBi(40 nm)/LiF(1 nm)/Al(100 nm). The weight ratio of green-QDs to red-QDs (G:R) and the total concentration of the mixed QDs solution (corresponding to the thicknesses of the mixed QDs layer in device-W) are both changed to optimize the performances of the devices. Here, we just present three typical samples to illustrate the optimization process. The G:R and total concentration of the mixed QDs solution for devices W1, W2, and W3 are 1:5 with 3.2 mg/ml (0.51 ML), 1:5 with 3.9 mg/ml (0.62 ML), and 1:4 with 4.2 mg/ml (0.67 ML) respectively. The normalized EL spectra of the device-W at 7 V bias are shown in Fig. 3(a).

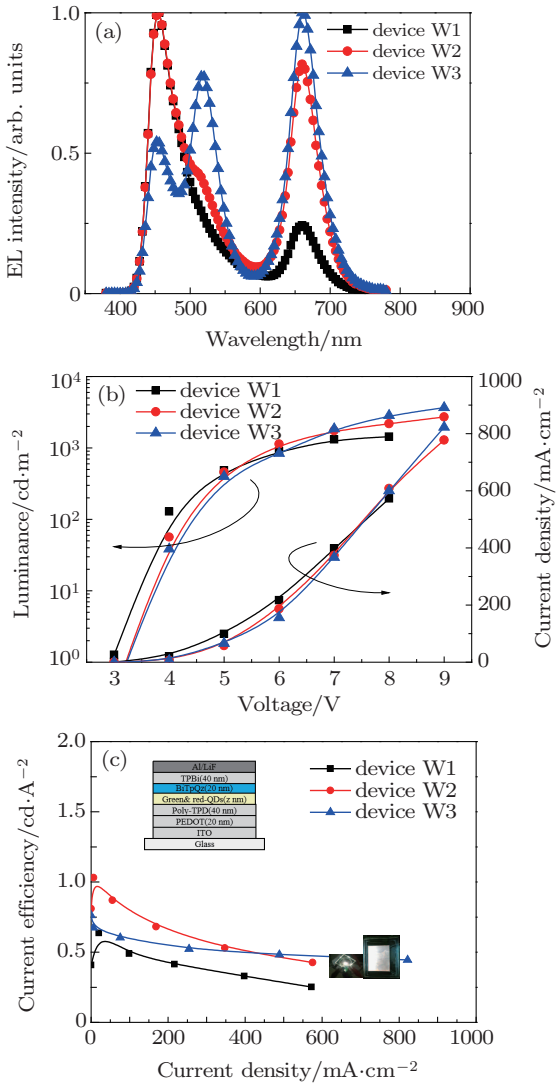


Fig. 3. (color online) (a) Normalized EL spectra of device-W under a bias of 7 V, in which the weight ratio of G:R and the total thickness values of the mixed QDs layers for devices W1, W2, and W3, are 1:5 with 0.51 ML, 1:5 with 0.62 ML, and 1:4 with 0.67 ML respectively. (b) *L*–*V*–*J* and (c) current efficiency–current density of devices-W with upper inset: device structure of the device-W, below-left inset: photo of the 3 mm×3 mm active area emitting device-W3 at 7 V, and below-right inset: photo of 2.1-inch (1 inch = 2.54 cm) white QLED at 8 V.

It can be seen from Fig. 3(a) that the device-W1 (G:R = 1:5, 0.51 ML) shows two peaks at 456 nm (BiTpQz) and 660 nm (red-QDs) with imperceptible green-QDs emission. With increasing the thickness of the mixed QD layer, device-W2 (G:R = 1:5, 0.62 ML) shows two peaks at 456 nm (BiTpQz) and 660 nm (red-QDs) with a shoulder at 516 nm (green-QDs). Then, as the ratio of G to R and the concentration of the mixed QDs solution increase to 1:4 and 4.2 mg/ml, the device-W3 (G:R = 1:4, 0.67 ML) shows three peaks at 516 nm (green-QDs), 660 nm (red-QDs) and a suppressed blue emission of 456 nm (BiTpQz). It indicates that the intensities of blue emission can be adjusted by varying the thickness of QD layer in these devices, which agrees with the results of Fig. 2. Figures 3(b) and 3(c) show the *L*–*V*–*J* and the current efficiency–current density characteristics of device-W respectively. It can be seen from Fig. 3(b) that the current density of

device-W changes little within the error as the thickness of the mixed first EML changes from 0.51 ML to 0.67 ML. The turn-on voltage and the maximum brightness of device-W increase with the thickness of the mixed QDs increasing. Although the device-W2 exhibits the best current efficiency in Fig. 3(c), the optimized device with the best spectral characteristics for white-QLED is obtained from device-W3 (Fig. 3(a)), which exhibits a turn-on voltage of 3.2 V, a maximum brightness of 3660 cd/m^2 at a bias of 8 V (Fig. 3(b)), and the CIE 1931 chromaticity (0.27, 0.23)–(0.29, 0.41) from 4 V–8 V (inset of Fig. 4(b)) which are in the region of white light. The below-left inset of Fig. 3(c) shows the photograph of the white-QLED recorded at 7 V, demonstrating the bright and uniform white emission. We finally realize a 2.1-inch white-QLED prototype by the same method (the below-right inset of Fig. 3(c)) which implies a good stability of the white-QLED.

In order to prove that the blue emission in our white-QLED comes from BiTpQz instead of Poly-TPD, a corresponding device without BiTpQz is fabricated based on the structure (the inset of Fig. 4(a)) of ITO/PEDOT:PSS(20 nm)/poly-TPD(40 nm)/green-QDs:red-QDs(G:R = 1:4, 0.67 ML)/TPBi(40 nm)/LiF(1 nm)/Al(100 nm), in which all the layers are the same as that of device-W3 except BiTpQz. Figure 4(a) shows the normalized EL spectrum of the corresponding device at 7 V, which exhibits a spectrum with green-QDs (516 nm) and red-QDs (660 nm) emission but without the distinct blue emission. It indicates that the blue emission from Poly-TPD can be ignored in our device.

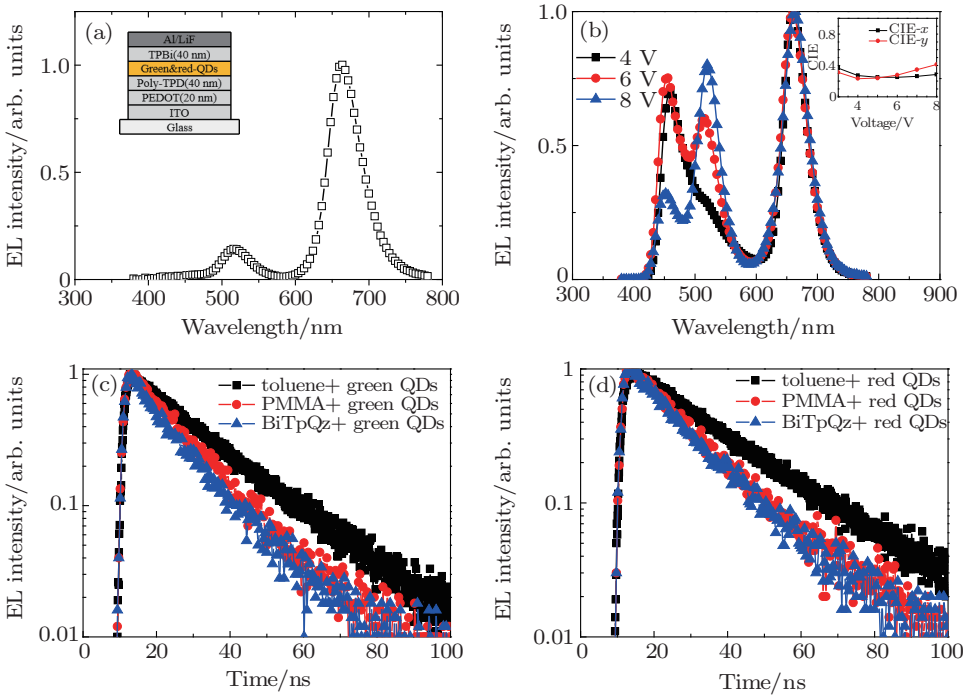


Fig. 4. (color online) (a) Normalized EL spectrum of corresponding device with a structure in which all the layers are the same as those of device W3 except BiTpQz, and the device structure in inset. (b) Normalized EL spectra of device-W3 at the voltages varying from 4 V to 8 V, and corresponding CIE trend chart in inset. The PL lifetimes of QDs in toluene solution, QDs/PMMA blend film, and QDs/BiTpQz blend film for (c) green-QDs and (d) Red-QDs.

Excitations of the QDs in QLEDs occur via either direct charge injection and/or nonradiative energy transfer (NRET) from an adjacent charge transport layer.[24,25] The overlaps of the QD absorption spectrum with the PL spectra of BiTpQz (as shown in Fig. 1(a)) imply the possibility of excitation mechanism via the Forster energy transfer from BiTpQz to QDs. However, taking into account the white QLED energy band structure (Fig. 1(b)) and the spectrum results of device-W3 at low voltage (Fig. 4(b)), the charge injection is the most likely way to generate an exciton instead of the Forster energy transfer. In order to verify the operation process in our white-QLEDs, the normalized EL spectra of the optimized device-W3 at the applied voltage varying from 4 V to 8 V are presented in Fig. 4(b). At a bias of 4 V (just above a turn-on voltage of 3.2 V), the spectra in Fig. 4(b) show two peaks of red-QDs and BiTpQz each with a weak shoulder of green-QDs. As the voltage increases, the blue emission from BiTpQz decreases, and the green and red emission from QDs increase gradually. Since the carrier mobility in QDs is quicker than in BiTpQz, increasing voltage can cause excitons to recombine further into organic layer and farther away from QDs,[13] which does not favor the Forster mechanism since exciton energy transfer to QDs occurs within the Forster radius. However, the QD emission is more efficient at higher voltages in the device as shown in Fig. 4(b). This result suggests that the Forster energy transfer from BiTpQz to QDs is not the dominant excitation process of QDs in our hybrid white-QLEDs. Instead, charge injection appears to be an important mecha-

nism of EL in QDs.

In order to support the proposed excitation mechanism in our device, we further investigate the influence of BiTpQz on PL lifetime of the QDs via TRPL. The fluorescence decay curves of the QDs in toluene solution, QDs/PMMA blend film, and QDs/BiTpQz blend film are measured at the QD peak emission. The results of the green-QDs and red-QDs cases are shown in Figs. 4(c) and 4(d), respectively. Previously, it has been proved that the fluorescence lifetime of the acceptor QDs increases due to the exciton feeding via NRET.[26] However, in our work, little difference between the fluorescence lifetimes of QD in QDs/PMMA and QDs/BiTpQz film is observed from both the green-QDs and red-QDs cases. For the green-QDs, figure 4(c) shows a single exciton lifetime of 19 ns in toluene solution and a reduced lifetime of 13.81 ns in QDs/PMMA film. The reduced lifetime of QDs in film can be attributed to the involvement of the nonradiative process between packed QDs and/or the exposure of the dipole to an inhomogeneous environment. Meanwhile, a slightly reduced lifetime of 12.77 ns in the QD/BiTpQz film compared with that of QDs/PMMA film is observed. For the red-QDs, figure 4(d) shows the same trend as Fig. 4(c). The red-QDs exhibit exciton lifetimes of 23 ns in toluene solution, 16.25 ns in QDs/PMMA film, and 15.42 ns in QD/BiTpQz film, respectively. Compared with that of QDs/PMMA film, a slightly reduced lifetime of QDs in QD/BiTpQz film can be ascribed to the probable charge separation between QDs and BiTpQz.[27] However, since the enhanced fluorescence lifetime of QDs has been observed from neither green-QDs/BiTpQz nor red-QDs/BiTpQz films, the excitation mechanism of QDs in our white-QLEDs cannot be ascribed to the energy transfer from BiTpQz to QDs.

4. Conclusions

We demonstrate a bright white-QLED with a blue fluorescent material BITpQz deposited on a thin film of mixed green- and red-QDs serving as bilayer EML. The optimized white-QLED exhibits a turn-on voltage of 3.2 V and the maximum brightness of 3660 cd/m^2 @8 V with the CIE chromaticity in the region of white light. The analyses of EL spectral and TRPL show that charge injection is the dominant excitation process of the ultra-thin layer of QDs in our white-QLEDs.

References

[1] Zhong X H, Xie R G, Zhang Y, Basche T and Knoll W 2005 *Chem. Mater.* **17** 4038
[2] Sun Q J, Wang Y A, Li L S, Wang D Y, Zhu T, Xu J, Yang C H and Li Y F 2007 *Nat. Photon.* **1** 717
[3] Cheng G, Mazzeo M, Rizzo A, Li Y Q, Duan Y and Gigli G 2009 *Appl. Phys. Lett.* **94** 243506
[4] Li Y P, Liu K, Lu S D, Yue S Z, Chi D, Wang Z J, Qu S C and Wang Z G 2015 *Nanoscale* **7** 17283
[5] Colvin V L, Schlamp M C and Alivisatos A P 1994 *Nature* **370** 354
[6] Kwak J, Bae W K, Lee D, Park I, Lim J, Park M, Cho H, Woo H, Yoon D, Char K, Lee S and Lee C 2012 *Nano Lett.* **12** 2362
[7] Lee K H, Lee J H, Kang H D, Park B, Kwon Y, Ko H, Lee C, Lee J and Yang H 2014 *ACS Nano* **8** 4893
[8] Dai X L, Zhang Z X, Jin Y Z, Niu Y, Cao H J, Liang X Y, Chen L W, Wang J P and Peng X G 2014 *Nature* **515** 96
[9] Anikeeva P O, Halpert J E, Bawendi M G and Bulovi V 2007 *Nano Lett.* **7** 2196
[10] Kang B H, Seo J S, Jeong S, Lee J, Han C S, Kim D E, Kim K J, Yeom S H, Kwon D H, Kim H R and Kang S W 2010 *Opt. Express* **18** 18303
[11] Tan Z N, Hedrick B, Zhang F, Zhu T, Xu J, Henderson R H, Ruzyllo J and Wang AY 2008 *IEEE Photon. Technol. Lett.* **20** 1998
[12] Kang B H, You T Y, Yeom S H, Kim K J, Kim S H, Lee S W, Yuan H, Kwon D H and Kang S W 2012 *IEEE Photon. Technol. Lett.* **24** 1594
[13] Torriss B, Hach A and Gauvin S 2009 *Org. Electron.* **10** 1454
[14] Wu W, Li F S, Nie C, Wu J Q, Chen W, Wu C X and Guo T L 2015 *Vacuum* **111** 1
[15] Ding L, Li H K, Zhang M L, Chen J and Zhang F H 2015 *Chin. Phys. Lett.* **32** 107805
[16] Fan C J, Wang R X, Liu Z, Lei Y, Li G Q, Xiong Z H and Yang X H 2015 *Acta Phys. Sin.* **64** 0167801 (in Chinese)
[17] Bae W K, Char K, Hur H and Lee S 2008 *Chem. Mater.* **20** 531
[18] Ji W Y, Jing P T, Zhao J L, Liu X Y, Wang A and Li H B 2013 *Nanoscale* **5** 3474
[19] Cho J, Jung Y K and Lee J K 2012 *J. Mater. Chem.* **22** 10827
[20] Yang X Y, Zhao D W, Leck K S, Tan S T, Tang Y X, Zhao J L, Demir H V and Sun X W 2012 *Adv. Mater.* **24** 4180
[21] Qian L, Zheng Y, Xue J G and Holloway P H 2011 *Nat. Photon.* **5** 543
[22] Kagan C R, Murray C B and Bawendi M G 1996 *Phys. Rev. B* **54** 8633
[23] Caruge J M, Halpert J E, Bulovic V and Bawendi M G 2006 *Nano Lett.* **6** 2991
[24] Lee K H, Lee J H, Song W S, Ko H, Lee C, Lee J H and Yang H 2013 *ACS Nano* **7** 7295
[25] Mutlugun E, Guzelturk B, Abiyasa A P, Gao Y, Sun X W and Demir H V 2014 *J. Phys. Chem. Lett.* **5** 2802
[26] Kagan C R, Murray C B, Nirmal M and Bawendi M G 1996 *Phys. Rev. Lett.* **76** 1517
[27] Jing P T, Yuan X, Ji W Y, Ikezawa M, Liu X Y, Zhang L G, Zhao J L and Masumoto Y 2011 *Appl. Phys. Lett.* **99** 093106